Chapter 2 – Literature review on LS PMSM technology

This chapter focuses on LS PMSM machine operation, previously designed LS PMSM machines and unique studies done in the past. The review will also include studies on various topologies and the lessons learnt in each. Similar studies done by others will also be compared to formulate a better understanding of the components unique to an LS PMSM. The goal of this chapter is to aid in the rotor design for the LS PMSM prototype.

2.1 Introduction

An LS PMSM machine is a high efficiency synchronous machine, which operates with fixed line voltage and frequency, thus making it ideal for IM replacement [16]. In comparison to an IM, this machine has a higher power factor, lower losses at steady state operation, lower thermal operating temperature and greater power density [16, 17]. This machine concept first made its appearance in the late 1970s but was referred to as PM motors with line-starting capabilities [16-19]. From these early articles the machines basic construction and operation methodology was defined.

LS PMSM machine technology only became a popular industry topic over the past couple of years with the introduction of the super premium IE 4 machine standard. This standard was proposed by the International Electrotechnical Committee (IEC) in 2008 along with standard efficiency (IE1), high efficiency (IE2) and premium efficiency (IE3) [30]. The purpose of the IE4 standard in 2008 was purely informative as there was insufficient technological information available as there was no commercial manufactured machine to meet this standard. Some of the machine manufacturers stated that it would not be technically feasible to reach this level of efficiency with IM technology. At that stage, very high efficiency PMSMs started entering the industrial market which had the efficiency capabilities surpassing that as required by IE4 [30]. Thus it was clear new research and development had to be done in PMSM technology, whether it was a line-fed machine or drive controllable.

The IE machine standard focuses on the five different types of losses associated with electrical machines. Those losses are as follow:

- Stator I^2R losses (± 25% – 55 %)
- Rotor I^2R losses (± 20 %)
- Stray load losses (± 2% - 15%)
- Core Losses (± 20 %)
- Winding and friction losses (± 1% – 10%)

The percentage of losses is influenced by the machine's power rating. To make a machine more efficient, improvement in one or more of these areas is needed. An example of this would be to reduce the rotor losses or completely eliminate them, as is the case of an LS PMSM. By eliminating the rotor cage losses at rated speed, the efficiently of a machine will rise [13, 23, 30]. As an IM's efficiency is directly linked to the percentage of maximum load, the machine's efficiency will decrease as the load increases. This is attributed to a rise in stator current due to larger power demand resulting in higher rotor cage losses. With an LS PMSM, the efficiency rises as the load increases [13]. Figure 2.1 below is the loss breakdown of a typical four-pole, 50 Hz IM at steady state. In the figure the losses due to the cage can be seen clearly as being one of the biggest influences on machine efficiency.

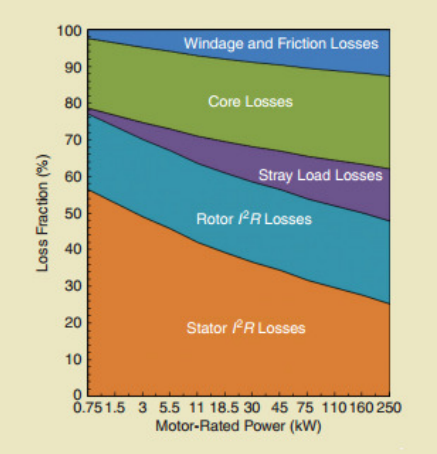

Figure 2.1: Typical losses of a four-pole IM [31].

To calculate the efficiency of a machine in which the rotor cage losses is removed, one has to use the following two equations [30]:

$$\eta_{new} = 10^4 \eta_{orig} [10^4 + \Delta p_{total} (10^2 - \eta_{orig})]^{-1}$$
$$\Delta p_{total} = 10^{-2} [\sum_{l=1}^{5} p_{compl}] \Delta p_{compl} \qquad (2.1)$$

with η_{new} the new rated efficiency, η_{orig} the original efficiency, Δp_{total} the total losses, l is the loss component and Δp_{compl} is the variation of the loss component. All the variables are a function of percentage. As with the IM, the LS PMSM also has a theoretical efficiency limitation. If one assumes the stator core and windings are optimised, the LS PMSM is only limited by the rotor design for this machine.

An LS PMSM rotor has two critical components that it needs to function. The rotor must contain a form of a damper or cage winding and permanent magnets. Figure 2.2 contains one of the four basic LS PSMS rotor configurations. In this configuration the PMs are situated deep inside the rotor beneath the cage winding. This rotor contains no flux barriers and is merely to illustrate the concept. The PMs are the green blocks and the arrows indicate the direction of the polarisation.

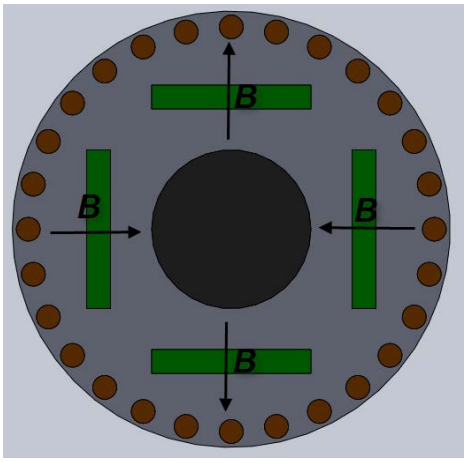

Figure 2.2 Basic embedded PM LS PMSM rotor

The purpose of the cage windings is to provide the transient torque for the machine. The cage however produces no torque once the machine reaches synchronous speed because the cage bars are stationary with respect to the revolving synchronous stator field. This eliminates the cage rotor losses of the machine at steady state because there are no induced currents in the bars [10]. The cage is the main torque producing component during transient state and causes the machine to overcome the magnetic braking torque and to accelerate the rotor to synchronous speed.

Once the rotor reaches synchronous speed, the machine operates as a PMSM as the PMs magnetic flux synchronises with the revolving stator field. At this point the synchronised PMs produce the torque. The speed of the motor at steady state will not vary as the load increases or decreases; this is a further advantage an LS PMSM has over an IM. During transient period the PMs generate what is defined as braking torque. This torque has a negative effect on the machines start-up performance and the magnitude of this negative torque component is dependent on the magnet volume [20, 21]. If the braking torque generated by the magnet is too big the rotor will not synchronize [10].

Figure 2.3 shows the LS PMSMS torque curve. During the transient period the asynchronous torque (T_{asy}) is the result of the interaction between the cage torque (T_c) and braking torque (T_m). Both the braking torque and cage torque are dependent on the individual component design. At steady state, the synchronous torque (T_{syn}) is mainly produced by the PM alignment torque but depending on the rotor topology. There can also be a reluctance torque component depending on the rotor topology. The performance of the machine is greatly influenced by the interaction between the cage and PMSM topology [10, 20].

From Figure 2.3 it is not clear at which point the machine synchronizes. Synchronization is possible at a point near rated speed and varies depending on the load connected to the machine as well as the design. Thus once this point is reached the machine is pulled into synchronism by the PM alignment torque.

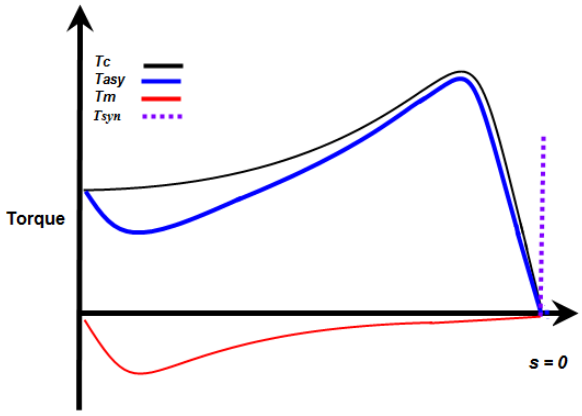

Figure 2.3: LS PMSM theoretical torque curve [10]

The braking torque contributes to the biggest drawback of an LS PMSM. This reduces the starting torque and the torque profile during the transient period of the machine. This impacts the loading capabilities and load inertia of an LS PMSM to reach synchronism [22, 23]. The braking torque phenomena in the machine was first investigated by Honsinger in 1980 [19], and his work form the basis of the concept behind it.

Several comparison studies between IMs and LS PMSMs have been done over the last couple of years. In 2009, Isfahani and Vaez-Zedeh concluded from their study in [23] that an LS PMSM has superior performance over an IM with regards to pump, fan and compressor loads (constant speed with long operating cycle type loads). They found that an LS PMSM had higher efficiency, power factor and torque density and its operating temperature is lower than the IM due to the absence of rotor bar currents. Although these machines' initial cost is higher than an IM, the cost of ownership is much less, making it a very attractive machine for certain applications. The drawback of this machine is however its starting torque and synchronisation capabilities which place limits on its application capabilities. Researchers over the past three decades have addressed several of the smaller issues with this machine which in turn made it possible to start manufacturing these machines at a larger scale for industry usage. For this machine to be truly competitive with IM, the issues with its starting transient behaviour and synchronisation capabilities need to be addressed.

One of the most recent studies was done by Mutize and Wang [18]. Although this paper was only presented after the initial literature survey was done the results were similar that listed in both [23] and [30] and indicating the relevance of further research in this field. For their study, they compared the two machines operation connected to a cooling fan application. The same stator was used and a retrofit LS PMSM rotor was designed, thus focusing on the influence on performance of rotor types. Although their study was only based on a 2D FEM analysis, the results were similar to that listed in both [23] and [30].

The performance focus was placed on both machines' transient and steady-state operations. They found that under steady state the LS PMSM had lower line current than the IM. During transient state the LS PMSM draws higher line current as this machine's rotor inertia is higher due to the braking torque component (fan loads have relative low inertia). This caused the IM to synchronize faster than the LS PMSM. Both machines' transient torque curves showed similar results. They conclude that although the LS PMSM had better efficiency and a higher power factor at steady state, the IM had better transient behaviour.

2.2 Designed and tested LS PMSM's

In this section LS PMSMs developed in the academic field will be discussed. All the designs in the section were verified by means of actual tests on the manufactured prototype. The machines selected for discussion each have a unique design.

2.2.1 Kuruhara-Rahman machine [21].

The Kuruhara-Rahman LS PMSM is a retrofit machine as it uses a 600W, four-pole IM stator. Figure 2.4 is a quarter machine sectional cut of this machine as well as the constructed rotor.

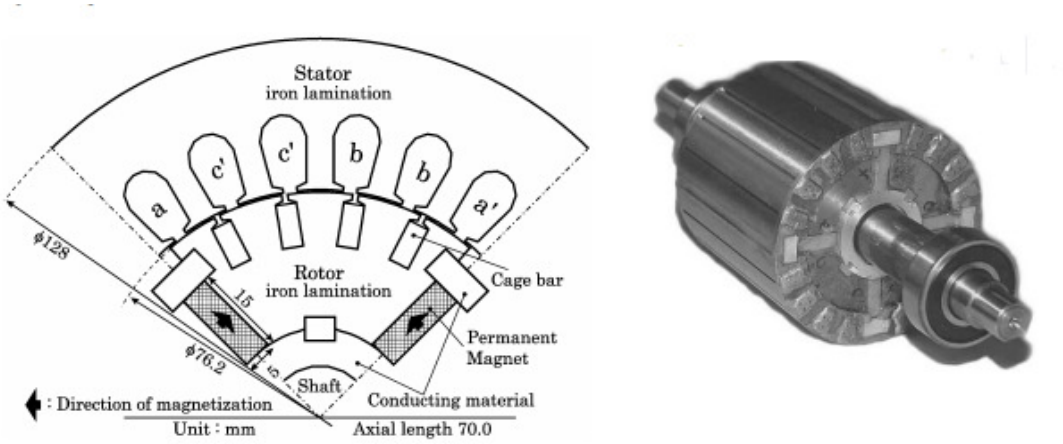

Figure 2.4: Kuruhara-Rahman LS PMSM design [21]

The prototype has three distinctive electromagnetic design features. The first is the tangential flux magnets. This technique utilises both sides of the PM to form the magnetic poles between two magnets and not over a magnet as in the case of the embedded radial flux topology. By using tangential flux topology, less PM material or lower grade magnets can be used to provide the same or even higher air gap flux density value as the more commonly used embedded radial flux topology [6]. The second feature is that the d-axis reluctance is larger than the q-axis reluctance. This is also acceded to the tangential flux topology. The difference in reluctance adds a large reluctance torque component to the machine. The last key feature is large pull-in torque obtained by the deep rotor bars. The rotor bars in a tangential flux

machine can span much deeper radial as the area behind the bars is much larger (except over the magnets) than with radial flux topology.

When focus is placed on the mechanical design the following needs to be known: one of the biggest drawbacks of this design topology is the leakage flux in the rotor at both magnet ends. To overcome this, this machine has a non-magnetic sleeve over the mild steel shaft. This eliminates the shaft end leakage flux. To eliminate the air gap end leakage flux, non-magnetic material was also placed to force the flux over the air gap. However the non-magnetic material is placed in such a way that a lamination still consists of one part and not four quadrants. This would add major mechanical difficulties.

To analyse the machine they used time stepping finite element analysis technique to predict the machine's operation. The machine model used in the analysis was an adapted 3D to 2D model that incorporated the end effect losses as well as the eddy current losses in the machine. The results obtained from the 2D analysis were then validated against the prototype. The two comparisons of note are the load performance and starting performance characteristics which were done against the original IM. A similar conclusion was made as in Section 2.1 regarding LS PMSM vs. IM. The prototype had more cogging torque than the IM. This is acceded to the rotor bars and magnets that are not skewed with respect to the stator. This can be eliminated by skewing the stator as it is very difficult to skew the LS PMSM rotor.

The most interesting point of note in this paper was the study done on rotor bar depth vs the maximum load inertia to synchronise the load. The simulation results show that as the rotor bar depth increases the maximum start up load also increases. The change in rotor bar depth had little or no effect on the efficiency of the machine as the rotor bars had no losses once the machine synchronized.

In 2010 Aliabad, Mojtaba and Ershad [32] proposed a new technique that could improve the operation of an LS PMSM. The Kuruhara-Rahman rotor design was used in their study. The focus point of the research was to improve the transient behaviour of the Kuruhara-Rahman by designing a stator specifically for an LS PMSM to reduce the braking torque induced in the machine by the PM during start up. The technique they suggested is stator pole changing. This technique entails that the stator is wound in such way that it could be switched from a two-pole to four-pole configuration once the rotor is the synchronisation of the four-pole machine. The technique works on the following basis with an LS PMSM: during normal start-up the stator and rotor have equal poles. The PMs in the rotor induces a voltage in the stator coils and the interaction between the induced voltage and stator current causes the braking torque. But by using a two-pole stator and a four-pole rotor the induced voltage is neutralized and in turn removes the braking torque, thus increasing the start-up torque and transient torque curve. As an IM rotor doesn't have a fixed pole, the cage of the rotor can be designed to provide optimal star-up torque for a two-pole machine with no limitations on the rotor resistance, as once the machine is synchronized at the rated speed of a four-pole machine the cage will have no effect on the torque production.

The redesigned stator LS PMSM performance was then compared to the results in [21]. In the course of the comparison the size of the magnets was also increased as there were no limitations on the magnet volume once the braking torque was eliminated by the pole changing stator. The increase in PM volume increased the steady state load capabilities. Table 2.1 below contains the results of the comparison.

Table 2.1: Performance comparison between IM, Kuruhara-Rahman and Aliabad-Mojtaba-Ershad LS PMSM's

	IM	**K-R Motor**		**A-M-E Motor**	
Input voltage (*V*)	200	130	140	190	190
Load torque (*Nm*)	4	3.82	3.82	5	6
Input current (*A*)	3.43	3.11	2.91	2.49	3.21
Power factor	0.688	0.981	0.986	0.987	0.996
Efficiency (%)	73.3	87.3	86.2	95.1	88.2
Rated Speed (*rpm*)	1434	1500	1500	1500	1500

The left column results for the Aliabad-Mojtaba-Ershad motor are for the same PM volume as in the Kuruhara-Rahman rotor and the right column results are for the increased volume. The conclusion of the research is that the disadvantaged transient behaviour of an LS PMSM can be overcome with this method and as a result the overall machine can be improved by adapting the original rotor design and the negative transient behaviour is eliminated.

2.2.2 Rodger-Lai machine [33]

The Rodger-Lai machine comprised two LS PMSM rotors with a centrifugal clutch between the rotors. The two rotors are labelled as the primary fixed rotor and the secondary rotor that is placed over the primary rotor shaft. The secondary rotor is held in place by the mechanical clutch. The idea behind the two part rotors is to neutralize the magnetic flux of the PMs that caused the braking torque during start up. This is done by aligning the two rotor segments as indicated in Figure 3.3 (a). Once the rotor reaches a speed close to synchronism, the mechanical clutch releases the secondary rotor and due to its low inertia it locks into place as indicated in Figure 2.5 (b). The advantage of using this technique is the same as with the Aliabad-Mojtaba-Ershad stator design. The cage of the machine can be designed to provide maximum start up torque whereas the PMSM component can be designed to provide maximum synchronous torque. With this configuration the cage will still act as a damper in the event of sudden load changes as the mechanical clutch will only release to normal once the rotor is near standstill.

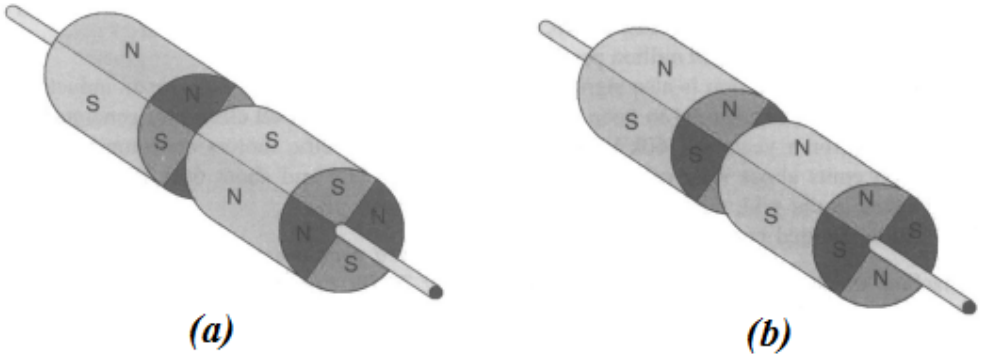

Figure 2.5: Rodger-Lai machine's operating principal a) start up configuration b) steady state configuration [33]

The biggest drawback with this design is the cost of manufacturing and the size of the machine. The twin rotor stack concept increases the axial length of the machine and in conjunction with the mechanical clutch, it also increases the manufacturing cost. The other issue is the reliability of the mechanical clutch over time.

In their presented paper the design constraints of an LS PMSM is clearly stated. By maximising the cage torque near synchronism (lower cage resistance) to ensure synchronisation the starting torque of the cage is decreased. When the synchronous torque capability is increased by increasing the reluctance or PM generated torque the possibility arises that the machine may not synchronise as the counter acting torque component is too big. Thus the relationship or ratio between optimal starting torque and synchronous torque is the key design focus point in conventional LS PMSM rotor design.

2.2.3 Chistelecan-Popescu machine [34]

The Chistelecan-Popescu machine is a claw pole modular design. A claw pole machine doesn't consist of laminations as one would find in standard IMs but out of modular unit stacked in a certain way to provide the needed pole configuration.

The Chistelecan-Popescu machine prototype consisted of both a rotor and stator design. The stator design utilised a pole changing technique similar to that used in [32]. They used a 2/4 starting/running coil configuration as well as switching from double star to delta once the machine was synchronised. The claw pole rotor consists of 4 modules which are rotated respectively to provide a form of skewing. Figure 2.6 a) contains half the claw pole rotor as well as the components. In Figure 2.6 b) the light purple represents the rotor cage, the blue and red the claw poles and the bright pink the ring shape PMs. As seen in the figure the cage bars are placed through the claws of the claw poles and the PM is placed between the two. The problem with this configuration is that only the PM poles are skewed with respect to the stator and the rotor bars are not skewed. This leads to higher time harmonics on the input current but reduces the cogging torque at rated speed.

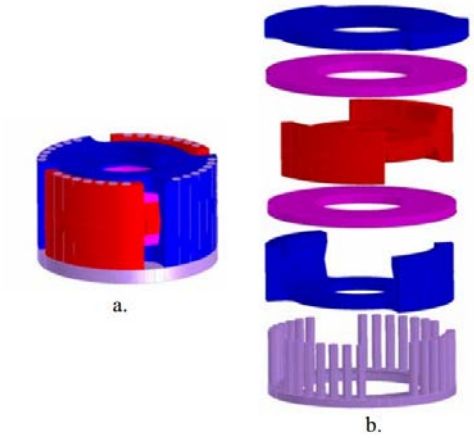

Figure 2.6: a) Half assembled claw pole rotor b) claw pole components

The paper that presents this machine only proves that it is capable of synchronising; it however provides no information regarding the load capacity of the machine, efficiency and power factor. The paper also lacks the information regarding the transient behaviour of the machine and thus no solid conclusion can be made regarding the feasibility of using this design. The main point of interest taken from this design is the pole changing technique used to counteract the magnetic forces generating the braking torque.

2.2.4 Weili-Xiaochen machine [35]

Weili-Xiaochen machine is a solid rotor machine. This differs from laminated rotors as the rotor stack consists of a solid magnetic metal. For the study the machine used a 6 pole 3-phase, 380 V, 30 kW IM stator. Figure 2.7 is a cross-sectional view of the machine.

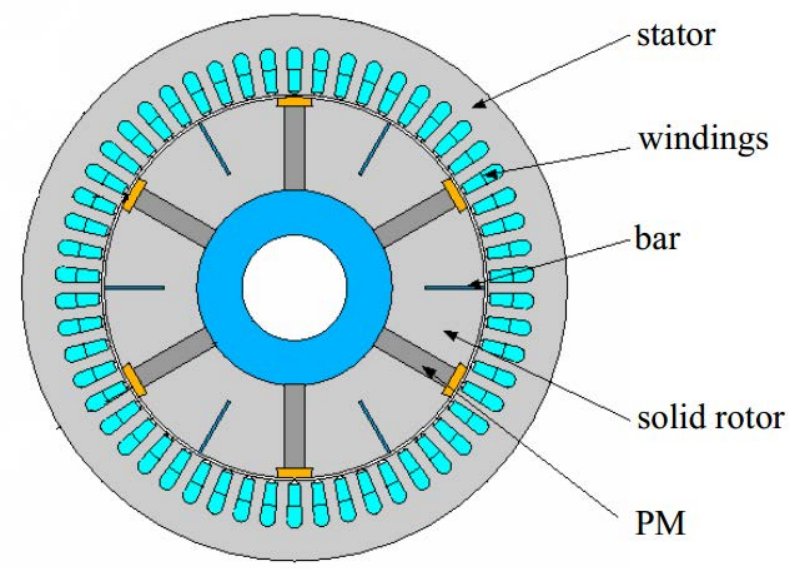

Figure 2.7: Section view of the Weili-Xiaochen machine [35].

The prototype machine was verified by comparing the calculated values against the tested values. The variables that were used in the verification process was the stator current, line voltage, output power,

power factor and efficiency. All the calculated values were within 2% of the actual tested values. It was also found that the applied load increases both the efficiency and the power factor improved significantly. This occurrence is in line with the results of other machine prototypes.

In [35] three influence studies were done. These studies are: the influence of load on machine performance, the influence of cage bar size on the operating performance and the influence of magnet size in the steady state performance. For the study on the influence of the bar size on the performance at steady state, the cage bar's width is varied. The influence on the input current and torque was inspected and it was found that as the bar's width increased the input was lower as the applied load increased. However this was not the case; with the maximum output the torque was the same. this is because the change in rotor cage resistance had no effect on the synchronous torque and only affected the transient operation.

For the magnet size influence study, two scenarios were explored. First the magnet height was kept constant and the magnet width was varied and in the second study the width was constant and the height varied. The affect on input current and output power was then inspected. Although in the paper it stated that in both instances the change had an effect on the two inspected parameters, the change was notably small (between 1% - 2 %).

2.3 **Rotor topologies study**

Selecting a suitable rotor topology for an LS PMSM is one of the key design decisions. The topology affects not only the performance of the machine but the material and manufacturing cost as well. Since an LS PMSM is a partial PMSM, the topologies used to design a PMSM can also be used in an LS PMSM. However not all topologies are suitable for an LS PMSM as the squirrel cage must also fit into the rotor core. Some topologies can be adapted to fit the cage.

In 2006, B. Singh et. al [11] presented a review article on the different rotor configurations for a PMSM rotor. It contained information on both radial and axial flux PMSM rotor topologies. With regards to radial flux machines, 23 different topologies were presented. Additionally [11] also contains a table categorising the 23 topologies in accordance with its type, advantages, limitations, power rating capabilities and applications.

The article states that al PMSM topologies can be defined under three categories: surface mounted, interior mounted and buried magnets. Surface mount magnets are glued onto the surface of the rotor and buried magnets are similar to that of surface mount. The difference is that the radial space between two magnets is not air but laminated iron material. Interior mounted magnets are place inside the rotor stack. Although [11] states that there are three topology categories, buried magnets can be seen as a surface

mount topology as the flux producing area of the magnet is at the surface of the air gap. Thus all PMSM rotor topologies can be categorized under surface mount magnets or interior/embedded magnets.

2.3.1 Surface mount magnets vs. interior magnets in PMSMs

In this section the two topologies will be discussed in depth, with more focus placed on the influence it has on a PMSM parameters and performance. This is to form a better understanding of the topology before taking the starting technique into account.

2.3.1.1 Surface mount magnets

Surface mount magnets are divided into two sub categories; surface mount magnets (SMM) and slotted surface mount magnets (SSMM). Both these topologies can provide very high air gap flux densities equal to that of the remanance (B_r) value of the permanent magnets used [5,10,11]. SMM rotors are the cheapest and simplest rotor topology. However, since the μ_r (1.04-1.05) of permanent magnets is very close to that of air ($\mu_r = 1$), the air gap as seen from both the rotor and stator sides tends to be larger than it actually is. If the PMs span the entire pole pitch of the rotor, the flux passes over the entire air gap; if the PMs do not span the entire pole pitch the magnetic flux only passes over the air gap in the areas where there are PMs. This is the case for both SMM and SSMM. Because the spaces between the magnets are filled with air, a SMM rotor is known as a non-salient pole machine [1]. With SSMM however the space between the two magnets are filled with laminated material. This causes a difference in reactance between the d and q axis of the rotor with X_q being larger that X_d. The difference in reactance adds a reluctance torque component which needs to be correctly integrated into the machine to increase the machine torque output [5,11]. The difference between reactance classifies the machine as a salient pole machine. Depending on the design of the SSMM, in some instances leakage flux can occur in the rotor; this was seen in some preliminary simulation results. Further investigation into this occurrence still needs to be done. Figure 2.8 is a representation of both SMM and SSMM.

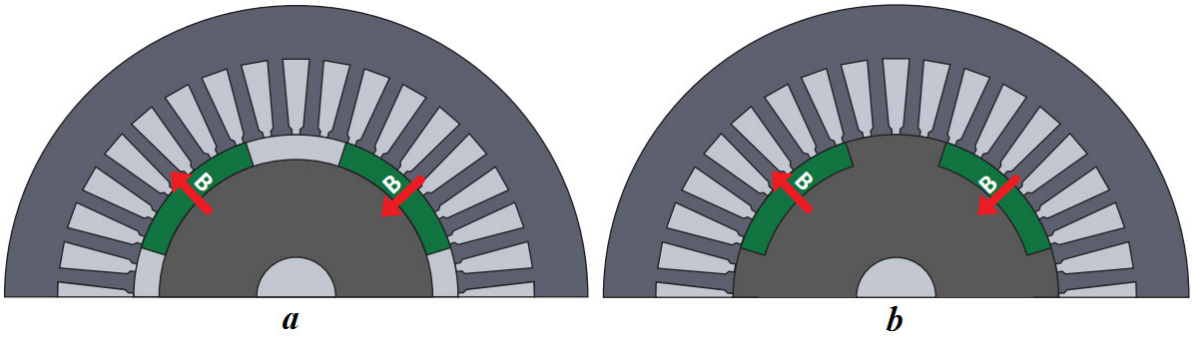

Figure 2.8: Surface mount magnets a) SSM b) SSMM [37]

One of the biggest disadvantages of surface mount magnets is the increased cogging torque and torque quality of the machine if the magnets are not correctly sized and placed [1, 10].

In the Figure 2.8 the PM area for both rotors is the same. The direction of the flux is indicated by the arrows. Another form of SMM topology is what is known as a Halbach magnetised rotor. This topology is mainly used in high speed motor applications. The Halbach array machine uses segmented PMs. The magnet array is indicated in Figure 2.9. Let the magnets of a four-pole SMM rotor span the entire rotor surface for explanatory purposes as in a). Divide all four magnets in equal parts and rotate one of the halves by 90° thus resulting in four magnets segments per pole as indicated by b). By dividing all eight segments again and rotating each second magnet by 45° c) is generated. This process can continue n^{th} time until theoretically an ideal Halbach array is obtained [38].

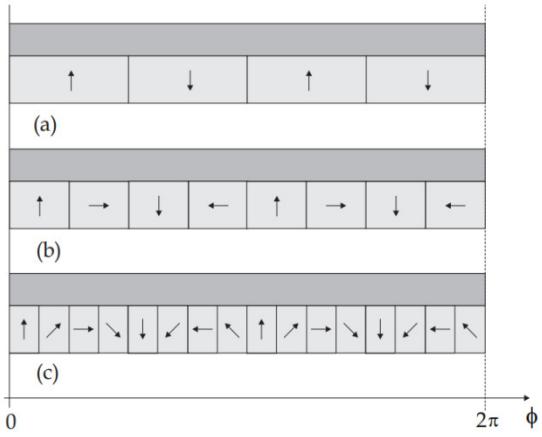

Figure 2.9: Representation of a Halbach array magnet configuration [38]

A Halbach array topology results in higher air gap flux density which if used correctly will increase the torque and power density of the machine. A close to sinusoidal air gap flux density waveform is also possible with this topology thus reducing torque ripple.

2.3.1.2 Embedded magnets

Embedded magnet topologies are divided into three sub categories, radial flux magnets (IRFM), circumferential flux magnets (ICFM) and embedded combination topology (ICT). As ICT is a combination of both IRFM and ICFM these two topologies will be discussed first. Figure 2.10 contains images of both topologies.

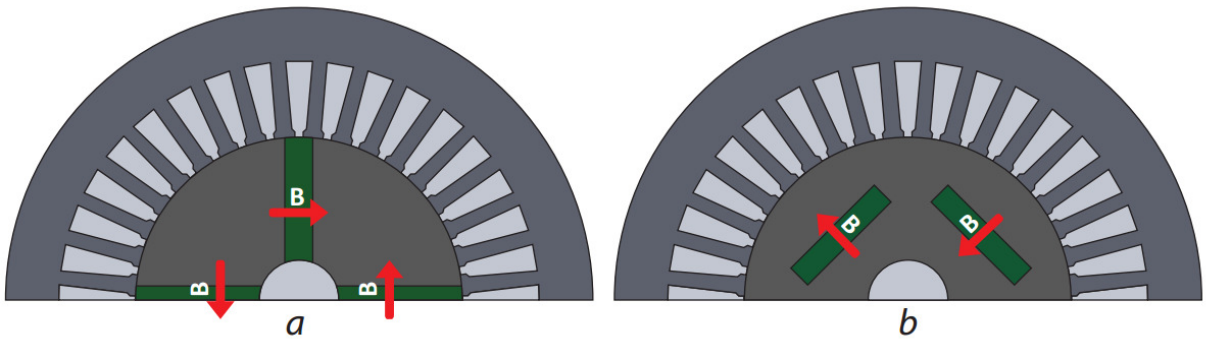

Figure 2.10: Embedded magnets topologies a) ICFM b) IRFM [37]

By placing the PM inside the rotor, the magnets are protected from any mechanical damage that can occur as well as possible demagnetisation. The other added advantage is that a very small air gap is possible.

The biggest disadvantage of embedded magnet topologies is the leakage flux inside the rotor. To overcome or reduce this problem, designers incorporate one of two techniques. The first is flux barriers and the second is saturation zones. Flux barriers reduce the leakage flux by forcing the magnetic flux towards the air gap. This technique also increases the reluctance in the machine. Flux barriers are slot that are added to the lamination and are filled with non-magnetic material or air. With IRFM, flux barriers are added as in Figure 2.12 on the magnet ends. The barriers in the figure are very basic and are roughly placed. The black contour line in both Figure 2.11 and Figure 2.12 provide information regarding the flux in the machine. The amount of flux lines in both figures is the same. In Figure 2.11 an increase in flux line in the back yoke is noted; this indicated an increase of flux crossing the air gap and a reduction in leakage flux.

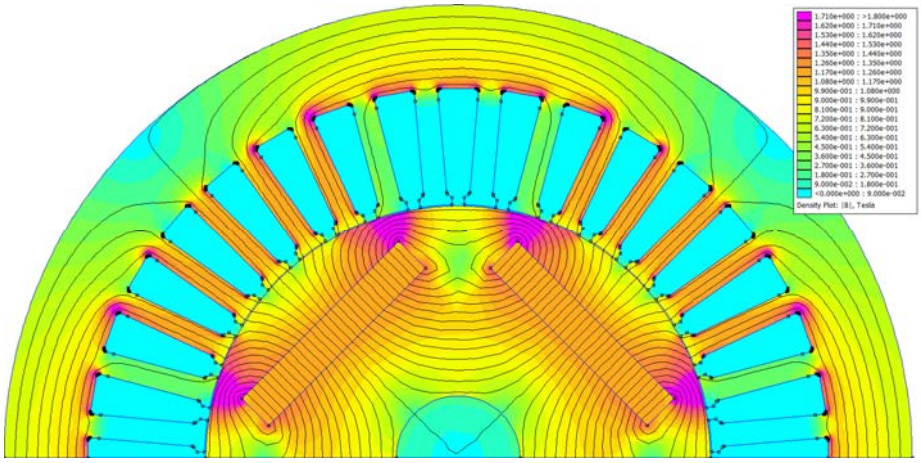

Figure 2.11: IRFM rotor with no flux barriers

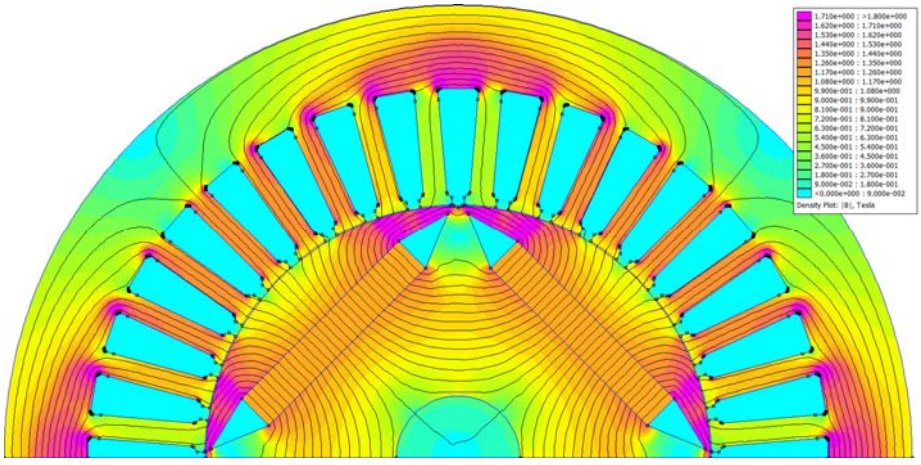

Figure 2.12: IRFM with flux barriers

In IRFM, like surface mount topologies, the pole flux distribution is dependent on the width of the magnet. A wider magnet provides a larger flux distribution over the air gap.

ICFM topology utilises flux forcing to form the magnetic poles in the machine. As with IRFM, this topology also has a large amount of leakage flux. This topology however is more complicated as the width of the magnets is placed in such a manner that flux is tangential to the radius of the machine. Figure 2.13 is an image of an ICFM indicating the leakage flux areas

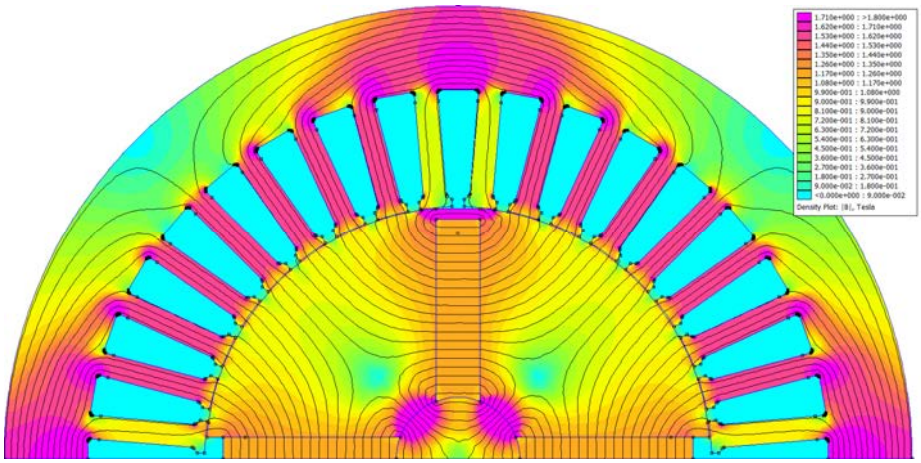

Figure 2.13: ICFM with leakage flux

As seen in Figure 2.13, the leakage flux areas are at the shaft and the end of the air gap end of the magnet. To eliminate the leakage flux through the shaft either a non-magnetic sleeve can be placed over the shaft or the shaft can be manufactured from a non-magnetic material [6]. In Figure 2.14, the mild steel shaft of Figure 2.13 is replaced by a non-magnetic material, stainless steel. Once again an increase in flux lines can be seen in the back yoke.

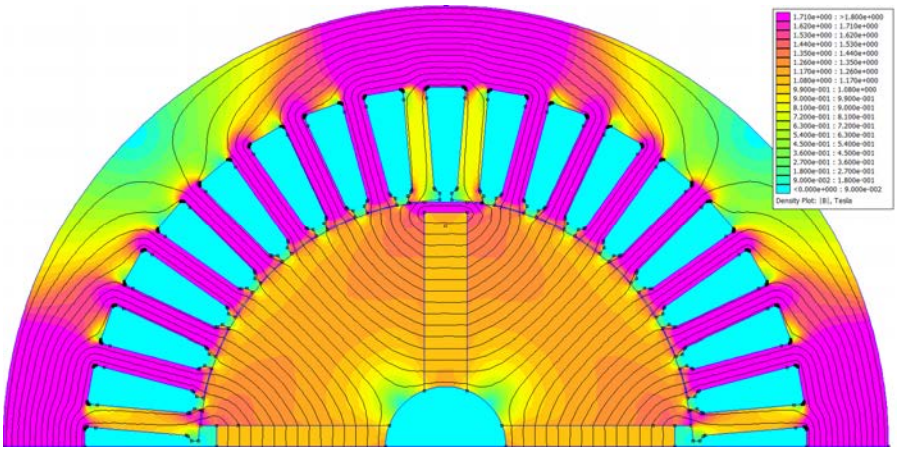

Figure 2.14: ICFM with non-magnetic shaft

To eliminate the leakage flux at the air gap end there are a couple of possible solutions. The first solution is to let the magnets span the entire radial length of the rotor. The problem with this method is that the rotor laminations are divided into separate pieces thus adding complications to the mechanical

manufacturing. The second technique is to incorporate saturation zone or magnetic saturation bridges. This technique is similar to adding flux barriers but for this technique, the material that the leakage flux flows through is forced into saturation thus limiting the amount of leakage flux [7]. The limiting of the leakage flux due to the saturation zones is a function both of the length and width of the material area that the leakage flux still flows through. This technique also ensures that a single lamination stack can be used to construct the rotor.

The biggest advantage of ICFM is the effect it has on the air gap. With this topology, a flux density value higher than that of the magnet's remanace value is possible [1, 6, 11]. Thus less PM material or a lower grade can be used to provide the same air gap flux density values as the other three topologies. Furthermore, the per pole flux distribution of this topology is not influenced by the length of the magnet as happens with surface mount magnets and IRFM.

Now that both IRFM and ICFM topologies have been addressed a closer look can be given ICT topologies. By definition if an embedded topology is a combination of IRFM and ICFM then it can be classified as ICT. Figure 2.15 contains four ICTs. There are however many more combinations possible and many more still to be designed and tested. One of the differences with ICT designs is the possible increase in the number of magnets needed as seen in (a) to (c).

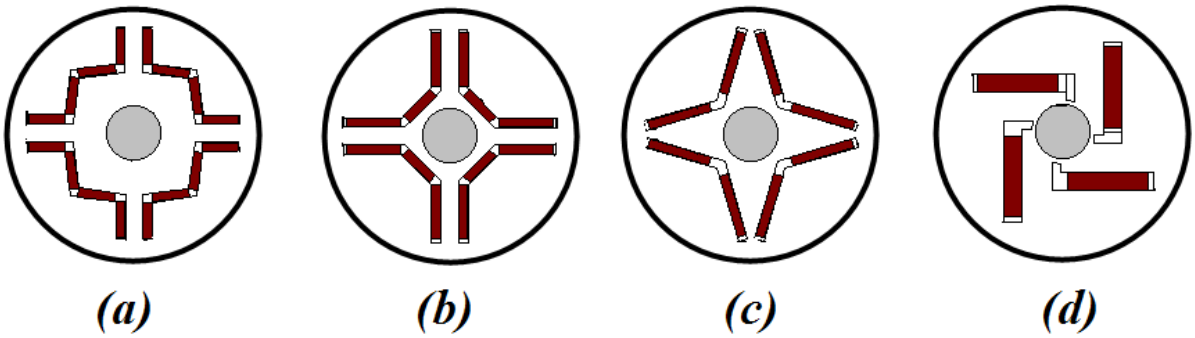

Figure 2.15: Examples of ICT [1, 11, 39, 40]

An ICT topology is used to address some of the issues with IRFM and ICFM. Some of these topologies tend to be more design intensive and can take longer to optimise. In Figure 2.15, (a) uses a much more complex layout than (d) however it is possible that both have the same performance. For all the above topologies the need for a non-magnetic shaft has been eliminated, but the need for flux barriers is still present, especially near the air gap end of the magnets.

In general, the main problem with all embedded topologies is the degree of difficulty to calculate the air gap flux [7]. This is due to the leakage flux of the machine that is always present. This makes the sizing of the PM much more difficult and the slightest change to the topology during the design can have a big effect.

2.4 Surface vs embedded magnets for LS PMSM

As an LS PMSM machine incorporates a type of squirrel cage to produce torque during the transient period, the placement of the cage affects the area available for the PMs and vice versa. As stated in Section 2.1 the interaction between the cage and PMs is one of the most important aspects when designing an LS PMSM.

When designing the rotor, one of the earliest decisions that must be made is the topology and more specifically, a surface mount magnet topology or embedded magnets topology. The decision influences not only the design process but the operation of the machine in both transient and steady-state operations.

In 2008 Huang, Mao, Tsai and Liu presented an article that investigated the effects of surface mount vs embedded magnets on the performance of an LS PMSM [10]. The article can be divided into two parts. In the first part an overview is given on the varies torque components and the influence it has on both states of the machine's operation irrespective of the selected topology.

In the second part a comparison study is done in an FEM package. The two rotors are both retrofit designs made for a 0.75 kW IM stator and use the same PMs in both designs. The two rotor designs are shown in Figure 2.16.

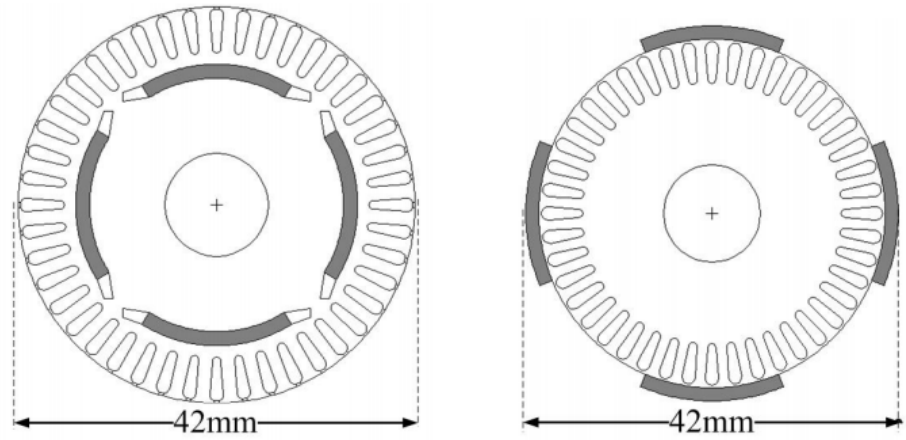

Figure 2.16: Rotors used for comparison study [10].

For the Embedded rotor design flux barriers were incorporated to reduce some of the leakage flux. The cage bars dimensions were also kept the same. To compare the two topologies the no load, synchronisation and synchronous operation were compared.

No Load:

Focus was placed on the flux density and distribution over the pole. The embedded magnets had a much lower air gap flux density value due to the leakage flux in the rotors. The difference between the two rotor's air gap flux density values is ± 25%. The higher air gap value of the surface mount magnets will in

turn increase the output power. The higher air gap flux density in conjunction with the span of the PMs will increase the reluctance force and ultimately add noise and vibration during operation. The surface mount rotor also had a higher cogging torque component of just over 2 Nm whereas the embedded magnet rotor's cogging torque is around 0.1 N.m

Synchronisation:

The synchronisation of an LS PMSM is affected by the cage and magnetic braking torque. If the braking torque component is too high the rotor will not synchronise when connected to certain loads. The braking torque of a machine is directly proportional to the back-emf induced by the magnets. Surface mount magnets tend to generate higher back-emf. The surface mount rotor induced a higher back-emf value which in turn reduced the synchronisation loading capability of the machine. Furthermore the embedded magnet rotor's settling time was much shorter.

Synchronous Operation:

To investigate the synchronous operation for the two rotors, the load was increased once the rotors were synchronised. The added load forced the embedded magnet design to desynchronise while the surface mount rotor did not. This is due to the higher air gap flux. Thus the assumption can be made that a high flux density during transient operation increased the braking torque and decreased the loading capability but once synchronised it provided higher maximum load. There is however no point in designing a machine that is capable of operating with high loads if the machine can't synchronize with a lower load.

When focus was placed on the line currents of the two machines, the embedded magnet rotor operating current was lower than that of the surface mount. This is due to the large synchronous reluctance component of the embedded magnet rotor.

To conclude the comparison study, Figure 2.17 is a barograph of the simulation results obtained.

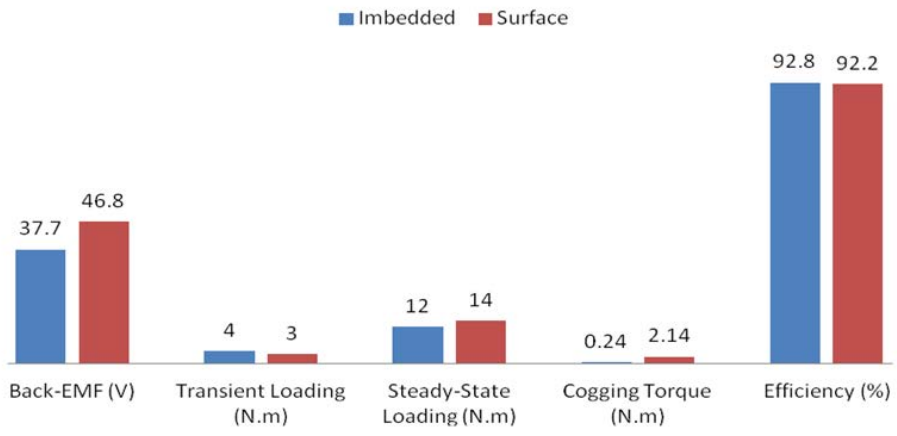

Figure 2.17: Comparison graph of surface mount magnets vs. embedded magnets [10].

Although the surface mount magnets rotor had slightly better synchronous loarding capability the embedded magnet rotor had much better transient operation results. Furthermore, by optimising the embedded magnet rotor by shifting the magnets closer to the air gap, better steady state operation can be achieved. Thus for an LS PMSM rotor an Embedded magnet design is a better option.

2.5 ICFM for an LS PMSM.

As there is a big difference between the IRFM topology and the ICFM topology, the affects of each when used in an LS PMSM need to be investigated. As stated earlier in the chapter, the air gap flux density of the LS PMSM is one of the key areas of the machine as it influences both the braking torque and the steady state torque. The air gap flux density value of the machine is influenced by the magnet size and the amount of leakage flux in the rotor. Over sizing the magnets to accommodate the leakage flux in the rotor poses a problem as the leakage flux is not necessary a constant value during the different stages of operation.

In 2006 Zhao, Li and Yan [6] presented an article investigating the affects of changing the PMs dimensions thus changing the volume of the magnets as well. The investigation was done on a four-pole configuration. One of the key remarks made in the article are the use of a non-magnetic shaft in the ICFM topology; this correlates to what was said in Section 2.3.1.2. In their study an increase of 0.45 T was gained. The second remark was that the leakage flux in the rotor is influenced by the air gap length of the machine. One of the interesting additional aspects they investigated was the pole pair number to air gap flux density value. As the number of pole pairs increased the magnet dimensions of the ICFM didn't need to be adapted as the magnet width is not affected by increase of pole. With this topology as the poles increase the air gap flux density value surpasses that of the of the remanance value of the magnet by 0.8 T. This proves the statement made in [11] that it is possible for the ICFM to produce above remanance flux density values in the air gap when the pole increases. In both [6] and [11], ICFM is not recommended for four-pole machines, as for the topology to be affective the pole arc width has to be smaller than the radial length of the magnet; however it could still be used.

The first study done in [6] was to determine the effect that the pole arc width coefficient has on the air gap flux density. This coefficient is the ratio between the magnetic pole arch width (τ_s) and the pole pitch (τ_p) as indicated in Figure 2.18. It was found that as the coefficient increase the flux density in the air gap decreases. The reason is that as the coefficient increased the PM width decreased which in turn increased the area of the lamination material facing the air gap. As the flux producing area of the magnet did not change but the air gap area increase a drop in flux density was expected. Furthermore, at the lower values of the coefficient, the air gap flux density value surpassed that of the remanance value of the magnets.

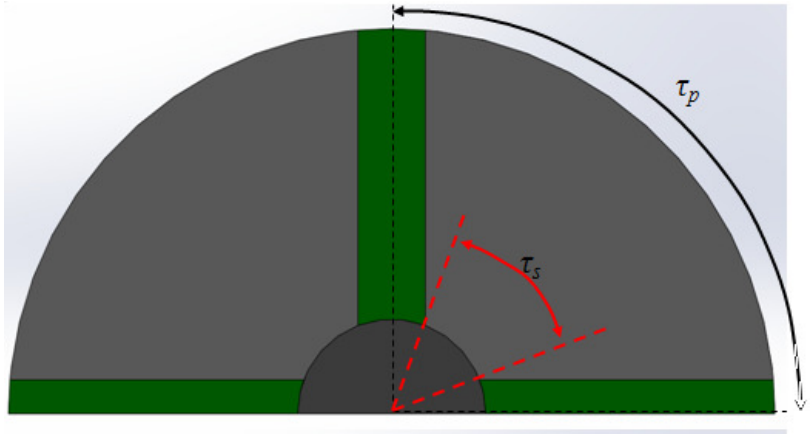

Figure 2.18: Determining the pole arch width [6,37]

The second study done was to increase the PM thickness. In theory, the increase in magnetic thickness provided an increase in mmf and the air gap flux density. This statement is only applicable to surface mount magnets and IRFM. However from the results obtained there was no increase in air gap flux density only in the per pole flux. With ICFM an increase in magnet thickness resulted in the decrease in the pole arch coefficient. This increased the air gap flux density but the per pole flux had almost no change.

No information was found on the effects a change in the radial length of an ICFM topology will have on the air gap flux density. Further investigation on this matter needs to be done. This issue and some other PM topology related aspects will be addressed in Chapter 3.

2.6 Torque components

Understanding the different torque components in an LS PMSM under the different stages of operation and understanding how the torque is generated will form a better understanding of the machine and aid in the design of one. The torque components discussed in this section are braking torque (T_m), asynchronous cage torque (T_{asy}), cogging torque and synchronous torque (T_{syn}).

2.6.1 Braking torque

The braking torque of an LS PMSM occurs during start-up and is a function of the back-emf and the slip of the machine [19]. At standstill the T_m is zero and increases to a maximum at low speeds after which it gradually decreases and becomes constant. Braking torque is produced in an LS PMSM in the transient period due to the induced current in the stator coils counter acting that of the input source. To calculate the braking torque V.B. Honsinger formulated in [12] the following equation:

$$T_m = \frac{3p}{\omega(1-s)}\left[\frac{R_1^2 + X_q^2(1-s)^2}{R_1^2 + X_q X_d(1-s)^2}\right]\left[\frac{R_1 E_o^2(1-s)^2}{R_1^2 + X_q X_d(1-s)^2}\right] \tag{2.2}$$

with p the pole pairs, R_1 the stator resistance, X_q and X_d the respective direct and quadrature axis reactances, E_o the RMS induced back-emf. The *abc* to *dq* transformation is discussed in Appendix A.

For a non-salient machine X_q and X_d is equal thus the first bracket will be equal to 1. Furthermore the product of the two brackets is equal to the short circuit stator copper losses.

The biggest influence factor on T_m, [20] states that as the back-emf is directly linked to the flux produced by the magnets. The placement of the magnets and shape has little or no effect on T_m as the inside of the rotor is not visible from an electromagnetic point of view from the stator during the transient period. This is because the high rotor current forms a saturated flux barrier. Even changing the relationship between X_d and X_q doesn't have as big on influence as the magnetic flux produced by the magnets. Thus the PM volume influences T_m the most. The effects of magnet's volume vs T_m and T_{asy} is shown in Figure 2.19.

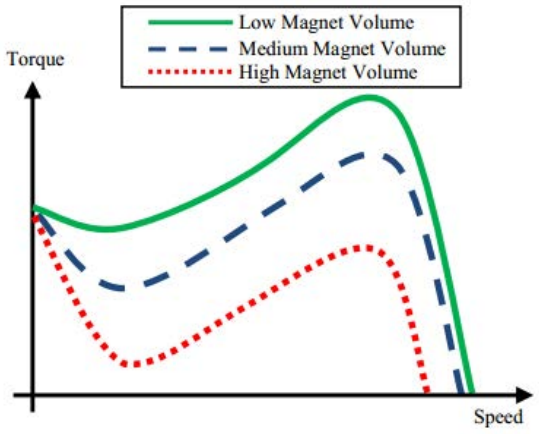

Figure 2.19: Influence of magnet volume on the torque curve [20].

Thus over sizing the PMs in the rotor will lead to the rotor not synchronising with or without load.

2.6.2 Asynchronous cage torque.

The asynchronous cage torque is directly linked to the cage design of the rotor. However the cage must be designed to provide optimum start up torque and a breakdown slip point close enough to synchronize. Furthermore the torque profile of the machine must be designed according to the type of load the machine is connected to [2]. From the literature it's clear that due to the load synchronization limitations an LS PMSM is ideal for pumps and fans [10, 31, 32]. These loads have zero torque at start-up and as speed increase the torque required to drive them increase. The torque required for a fan load is proportional to the square of the speed [18].

$$T_{fan} = T_{rated}\left(\frac{n}{n_{rated}}\right)^2 \tag{2.3}$$

In theory the load at zero speed is zero Newton-meter, however due to the load inertia the fan have a breakaway load that needs to be overcome. When designing the cage, this breakaway torque requirement must be kept in mind and not only the braking torque that needs to be overcome during starting. To calculate the starting torque of the machine the cage resistance (R_2) and the starting current is used [3]

$$T_{start} = \frac{3p}{\omega} I_{start}{}^2 R_2 \tag{2.4}$$

with the starting current calculated with

$$I_{start} = \frac{V_{line}/\sqrt{3}}{\sqrt{(R_1 + R_2)^2 + (X_1 + X_2)^2}} \tag{2.5}$$

Along with the starting torque, the maximum breakdown torque (T_{bd}) and the speed at which it occurs also plays a critical role in the transient period. If the breakdown torque point is at lower speeds the rotor connected to the load may not be able to synchronise. T_{bd} is influenced by the reactance of the machine and is calculated with

$$T_{bd} = \frac{3p}{2} \frac{V_{ph}}{\omega} \frac{1}{X_1 + X_2} \tag{2.6}$$

and occurs at

$$s_{bd} = \frac{R_2}{\sqrt{R_1{}^2 + (X_1 + X_2)^2}} \tag{2.7}$$

slip speed [3]. This point must be as close as possible to s = 1. However the closer s_{bd} is to s = 1, the lower the starting torque becomes [2, 3].

To calculate the torque generated by the cage during transient state the following equation is used

$$T_{asyn} \approx \frac{m_s V_{ph}{}^2}{\omega/p} \frac{R_2'/s}{\left(R_s + R_2'/s\right)^2 + \left(\omega L_\sigma\right)^2} \tag{2.8}$$

with R_2' the rotor resistance and L_σ total leakage inductance transposed to the stator reference frame [1].

2.6.3 Cogging torque.

Cogging torque is defined as the interaction of the rotor magnets with the stator teeth or poles and is independent of the stator current [5]. The interaction can be seen as the rotor aligning in a certain manner to the stator, a form of forced resting position. This is even present during the operation of the machine.

The amplitude of the cogging torque is influenced by the stator shoe design. If there are no slot openings then the result would be zero cogging torque. This however, will add complications to the stator coil winging procedure. Thus a fine balance is needed between slot opening and wire size. In general the slot opening is selected to be between two to three times that of the wire diameter. Even with a small slot opening, cogging torque is still present and this can have a negative effect on the machine. To counter the effect of cogging torque skewing is incorporated. In an IM, the rotor bars are skewed. This however is not that simple in PMSM and LS PMSM as the magnets segments can't be skewed and it is virtually impossible to produce individual laminations to skew the rotor bars if the magnets are segmented. To incorporate skewing in an LS PMSM the stator can be skewed [1, 3]

2.6.4 Synchronous torque.

At steady state operation the squirrel cage no longer produces torque. The torque produced by the machine is dependent on whether the machine is a salient or a non-salient rotor as the torque at synchronous speed is a combination of reluctance torque and electromagnetic torque, thus the synchronous torque is calculated

$$T_{syn} = T_{em} + T_{rel} \tag{2.9}$$

with

$$\begin{aligned} T_{em} &= \frac{m}{\omega}\frac{V_{ph}E_0}{X_d}\sin\delta \\ T_{rel} &= \frac{mV_{ph}^{\ 2}}{2\omega}\left(\frac{1}{X_q}-\frac{1}{X_d}\right)\sin(2\delta) \end{aligned} \tag{2.10}$$

and by combining the two torque components Equation 2.9 is rewritten as

$$T_{syn} = \frac{m}{\omega}\left[\frac{V_{ph}E_0}{X_d}\sin\delta + \frac{V_{ph}^{\ 2}}{2}\left(\frac{1}{X_q}-\frac{1}{X_d}\right)\sin(2\delta)\right] \tag{2.11}$$

with δ being the load angle in degrees [28]. If the rotor is non-salient the second term in the bracket is neglected as there is no reluctance torque present in the rotor. The electromagnetic torque is a function of

the back-emf and as the back-emf is influenced by the magnetic flux the higher the PM flux in the machine the higher the produced synchronous torque will be. However high PM flux in turn produces higher braking torque during the transient period

---

In this chapter information on the operation and past developed LS PMSM was provided and the features that is unique to each was identified. Different rotor topologies and the affect of each were compared to aid in the selection of a topology for the prototype. In the final part of this chapter the main torque components of an LS PMSM machine was discussed and information on the calculation is also provided.